Intrinsic cylindrical and spherical waves

2008 J. Phys. A: Math. Theor. 41 065401

(http://iopscience.iop.org/1751-8121/41/6/065401)

IOP PUBLISHING JOURNAL OF PHYSICS A: MATHEMATICAL AND THEORETICAL

J. Phys. A: Math. Theor. **41** (2008) 065401 (21pp) doi:10.1088/1751-8113/41/6/065401

Intrinsic cylindrical and spherical waves

I K Ludlow

Science and Technology Research Institute, University of Hertfordshire, College Lane, Hatfield, AL10 9AB, UK

E-mail: i.k.ludlow@herts.ac.uk

Received 11 November 2007, in final form 17 December 2007
Published 29 January 2008
Online at stacks.iop.org/JPhysA/41/065401

Abstract

Intrinsic waveforms associated with cylindrical and spherical Bessel functions are obtained by eliminating the factors responsible for the inverse radius and inverse square radius laws of wave power per unit area of wavefront. The resulting expressions are Riccati–Bessel functions for both cases and these can be written in terms of amplitude and phase functions of order v and wave variable z. When z is real, it is shown that a spatial phase angle of the intrinsic wave can be defined and this, together with its amplitude function, is systematically investigated for a range of fixed orders and varying z. The derivatives of Riccati–Bessel functions are also examined. All the component functions exhibit different behaviour in the near field depending on the order being less than, equal to or greater than $1/2$. Plots of the phase angle can be used to display the locations of the zeros of the general Riccati–Bessel functions and lead to new relations concerning the ordering of the real zeros of Bessel functions and the occurrence of multiple zeros when the argument of the Bessel function is fixed.

PACS numbers: 02.30.−f, 02.30.Gp

1. Introduction

Bessel functions are fundamental to our understanding of wave phenomena since they are solutions of the radial wave equation for problems having spherical and cylindrical symmetry [1, 2]. Numerous examples of their use have accordingly appeared in scientific and engineering literature concerning acoustic, elastic, electromagnetic and elementary particle waves [3–5]. The functions are written as $J_\ell(z)$, $Y_\ell(z)$ for cylindrical Bessel functions and $j_\ell(z)$, $y_\ell(z)$ for spherical Bessel functions, in which $z = kr$ where k is the propagation constant of the medium and r is the radial position of the wave. However, physical differences exist between cylindrical and spherical Bessel functions since their waves propagate, respectively, so as to obey inverse radius and inverse square radius laws for the wave power per unit area of wavefront. Hence it

follows that by eliminating the factors responsible for these differences, an intrinsic waveform will be obtained with properties that are of fundamental interest. The required transformations are

$$\text{intrinsic cylindrical wave:} \quad \varphi_\ell(z) = \sqrt{\frac{\pi z}{2}} J_\ell(z), \quad \chi_\ell(z) = \sqrt{\frac{\pi z}{2}} Y_\ell(z)$$

and

$$\text{intrinsic spherical wave:} \quad \varphi_{\ell+1/2}(z) = z\, j_\ell(z), \quad \chi_{\ell+1/2}(z) = z\, y_\ell(z),$$

where $\varphi_\nu(z)$, $\chi_\nu(z)$ are Riccati–Bessel (R–B) functions of order ν and the only difference now between the cylindrical and spherical R–B functions is that they have integer orders $\nu = \ell = 0, 1, 2, \ldots$ and half-odd integer orders $\nu = \ell{+}1/2 = 1/2, 3/2, 5/2, \ldots$, respectively. The modified functions satisfy the R–B differential equation and describe waves of constant power when z is real. Other types of intrinsic wave are also possible in which the order is neither integer nor half-odd integer and these have been used to describe wave propagation in media where the refractive index varies continuously as a mathematical power law in radius [5, 6].

A further important area of application of R–B functions is in inverse-scattering theory. This is concerned with a systematic study of the solutions and their properties for various scattering problems in nuclear, optical and acoustic physics. Examples of particular problems that have been examined are the derivation of the scattering amplitude from the differential scattering cross section and the construction of the scattering potential from the scattered phase shifts [7, 8]. In both cases it was assumed that scattering occurred at a spherically symmetric potential for particles of fixed energy that could be represented by scalar fields. The last condition clearly excludes light scattering at a sphere. Nevertheless in the case of a homogeneous sphere, a simple mathematical construction has been developed using R–B functions that uniquely inverts the Mie scattering coefficients to obtain the refractive index and radius of the particle [9].

The present paper examines how the intrinsic wave disturbance can be represented in a form that coincides with our physical intuition and gives an analysis of its properties for all positive and negative orders of ν when the wave variable z is real and positive. Comparisons are then be made between selected properties of the wave for fixed order when z is varied. The results clearly demonstrate a close interrelationship between cylindrical Bessel, spherical Bessel and R–B functions.

Extensive lists of the properties of cylindrical and spherical Bessel functions are given in standard mathematical handbooks such as [2]. The most important of these equations have been converted for R–B functions and the results are presented in the appendix.

2. Basic relations

The differential equation of R–B functions is

$$\left(\frac{\mathrm{d}^2}{\mathrm{d}z^2} + 1 - \frac{\mu_1}{z^2}\right) f_\nu^{(s)}(z) = 0, \qquad \nu = \ell + \delta$$
$$\text{for} \quad -1/2 < \delta \leqslant 1/2 \qquad \text{and} \qquad \ell = 0, \pm 1, \pm 2, \ldots. \tag{2.1}$$

Where $z = kr$ in which k is assumed to be a real propagation constant and r is the radial position relative to the origin, and $\mu_1 = \nu^2 - 1/4$. The label s has values 1– 4 and indicates the type of function: Riccati–Bessel $\varphi_\nu(z)$, Riccati–Neumann $\chi_\nu(z)$, Riccati–Hankel $\zeta_\nu^{(1)}(z)$ (outwards wave) and Riccati–Hankel $\zeta_\nu^{(2)}(z)$ (inwards wave), respectively, and ν is the order

of the function which is real but otherwise unrestricted. For a particular value of δ, a complete set of solutions of $\varphi_{\ell+\delta}(z)$ is generated for $\ell = 0, 1, 2, \ldots$. Specific symbols are used for the different types of functions and these are defined in terms of an intrinsic amplitude $M_\nu(z)$ and a spatial phase function $\theta_\nu(z)$ by

$$f_\nu^{(1)}(z) = \varphi_\nu(z) = M_\nu(z) \sin\theta_\nu(z) \tag{2.2a}$$

$$f_\nu^{(2)}(z) = \chi_\nu(z) = -M_\nu(z) \cos\theta_\nu(z) \tag{2.2b}$$

$$f_\nu^{(3)}(z) = \zeta_\nu^{(1)}(z) = -\mathrm{i}\, M_\nu(z) \exp \mathrm{i}\theta_\nu(z) \tag{2.2c}$$

$$f_\nu^{(4)}(z) = \zeta_\nu^{(2)}(z) = \mathrm{i}\, M_\nu(z) \exp -\mathrm{i}\theta_\nu(z). \tag{2.2d}$$

The derivative functions with respect to z are similarly defined:

$$\begin{aligned} \varphi_\nu'(z) &= N_\nu(z) \cos\phi_\nu(z) \\ \chi_\nu'(z) &= N_\nu(z) \sin\phi_\nu(z) \\ \zeta_\nu^{(1)\prime}(z) &= N_\nu(z) \exp \mathrm{i}\phi_\nu(z) \\ \zeta_\nu^{(2)\prime}(z) &= N_\nu(z) \exp -\mathrm{i}\phi_\nu(z). \end{aligned} \tag{2.3}$$

As z is real, the amplitudes $M_\nu(z)$ and $N_\nu(z)$ are both defined as real positive functions. Expressions for the new functions are

$$M_\nu(z) = \sqrt{[\varphi_\nu(z)]^2 + [\chi_\nu(z)]^2} \tag{2.4a}$$

$$\tan\theta_\nu(z) = -\frac{\varphi_\nu(z)}{\chi_\nu(z)} \tag{2.4b}$$

$$N_\nu(z) = \sqrt{[\varphi_\nu'(z)]^2 + [\chi_\nu'(z)]^2} \tag{2.4c}$$

$$\tan\phi_\nu(z) = \frac{\chi_\nu'(z)}{\varphi_\nu'(z)}. \tag{2.4d}$$

In addition, interrelations between the functions can be found from the Wronskian equation

$$W[\varphi_\nu(z), \chi_\nu(z)] = 1. \tag{2.5}$$

These are

$$M_\nu(z) N_\nu(z) \cos\Delta_\nu(z) = 1 \tag{2.6a}$$

$$M_\nu(z) = \frac{1}{\sqrt{\theta_\nu'(z)}} \tag{2.6b}$$

$$\phi_\nu(z) = \theta_\nu(z) + \Delta_\nu(z) \tag{2.6c}$$

$$N_\nu(z) = \frac{\sqrt{\theta_\nu'(z)}}{\cos\Delta_\nu(z)} \tag{2.6d}$$

$$\begin{aligned} \tan\Delta_\nu(z) &= -[\varphi_\nu(z)\varphi_\nu'(z) + \chi_\nu(z)\chi_\nu'(z)] \\ &= -M_\nu(z) M_\nu'(z) = \frac{1}{2}\frac{\theta_\nu''(z)}{[\theta_\nu'(z)]^2}. \end{aligned} \tag{2.6e}$$

Other useful expressions can be obtained by differentiation,

$$\begin{aligned} N_\nu'(z) &= \frac{\tan\Delta_\nu(z)}{N_\nu(z)} \left(1 - \frac{\mu_1}{z^2}\right) \\ \theta_\nu'(z)\, \phi_\nu'(z) &= \left(1 - \frac{\mu_1}{z^2}\right) \cos^2\Delta_\nu(z). \end{aligned} \tag{2.7}$$

3. Spatial phase angle, $\theta_\nu(z)$

A simple physical interpretation of (2.2*c*) is that it represents the profile of an outwards intrinsic wave in z-space of constant frequency at a fixed time. This consists of crests and troughs distributed between a source at the origin and infinity. Thus the amplitude $M_\nu(z)$ determines the heights and depths of the profile while the spatial phase angle $\theta_\nu(z)$ controls the locations at which the profile passes through its maxima, minima and zeros. Such a physical phase angle must therefore be both single valued and increase monotonically as the wave moves outwards from the source. Furthermore, it will be shown here that for all non-negative orders, the intrinsic wave has an initial phase angle of zero which ensures that $\varphi_\nu(z)$ has its smallest zero at the origin. In the far field, the intrinsic wave is approximated by a plane wave with

$$\theta_\nu(z) \underset{z\to\infty}{\simeq} z - \gamma_\nu^0 \qquad M_\nu(z) \underset{z\to\infty}{\simeq} 1, \tag{3.1}$$

where γ_ν^0 is a phase constant that depends only on ν.

A mathematical description of the wave, on the other hand, represents $M_\nu(z)\exp \mathrm{i}\theta_\nu(z)$ of (2.2*c*) by an Argand diagram with real and imaginary parts $-\chi_\nu(z)$ and $\varphi_\nu(z)$, respectively. Thus the phase angle is determined, in its most general form, by the multivalued function

$$\theta_\nu(z) = \tan^{-1}\left[-\frac{\varphi_\nu(z)}{\chi_\nu(z)}\right] \tag{3.2a}$$

obtained by inverting (2.4*b*). This phase can nevertheless be made single valued and brought into agreement with the physical property by restricting the angle to the positive half of the branch of (3.2*a*) that satisfies the initial condition

$$\theta_\nu(0) = 0; \qquad 0 \leqslant \nu. \tag{3.2b}$$

Complete expressions for $\theta_\nu(z)$ and $\phi_\nu(z)$ over the full range $0 \leqslant z < \infty$ then have the forms

$$\theta_\nu(z) = z - \gamma_\nu^0 + \gamma_\nu(z) \tag{3.3a}$$

$$\phi_\nu(z) = z - \gamma_\nu^0 + \gamma_\nu(z) + \Delta_\nu(z), \tag{3.3b}$$

where the latter relation is obtained by using (2.6*c*). Here $\gamma_\nu(z)$ is an auxiliary phase angle and $\Delta_\nu(z)$ is a phase shift. The different phase functions now have the following limiting values for far and near fields:

$$\begin{aligned} &\lim_{z\to\infty}\gamma_\nu(z) = \lim_{z\to\infty}\Delta_\nu(z) = 0 \\ &\lim_{z\to\infty}\theta_\nu(z) = \lim_{z\to\infty}\phi_\nu(z) = z - \gamma_\nu^0 \end{aligned}$$

and

$$\begin{aligned} &\lim_{z\to 0}\gamma_\nu(z) = \gamma_\nu^0 \\ &\lim_{z\to 0}\phi_\nu(z) = \lim_{z\to 0}\Delta_\nu(z) = a(\nu), \end{aligned} \tag{3.4}$$

where $a(\nu)$ is a constant that depends only on the magnitude of ν.

In the special case of $\nu = 1/2$, the above formalism leads to

$$\begin{aligned} &\varphi_{1/2}(z) = \sin z \qquad &&\chi_{1/2}(z) = -\cos z \\ &\zeta_{1/2}^{(1)}(z) = -\mathrm{i}\exp(\mathrm{i}z) \qquad &&\zeta_{1/2}^{(2)}(z) = \mathrm{i}\exp(-\mathrm{i}z) \end{aligned}$$

and

$$\begin{aligned} &\varphi'_{1/2}(z) = \cos z \qquad &&\chi'_{1/2}(z) = \sin z \\ &\left[\zeta_{1/2}^{(1)}(z)\right]' = \exp(\mathrm{i}z) \qquad &&\left[\zeta_{1/2}^{(2)}(z)\right]' = \exp(-\mathrm{i}z), \end{aligned} \tag{3.5a}$$

so that

$$\begin{aligned}\theta_{1/2}(z) &= \phi_{1/2}(z) = z\\ M_{1/2}(z) &= N_{1/2}(z) = 1\\ \Delta_{1/2}(z) &= \gamma_{1/2}(z) = a(1/2) = 0\end{aligned} \tag{3.5b}$$

and

$$\gamma^0_{1/2} = 0. \tag{3.5c}$$

4. The phase constant, γ^0_ν

The necessity for a phase constant follows directly from the existence of the recurrence relations of the R–B functions:

$$\begin{aligned}f^{(s)}_{\nu+1}(z) &= \frac{(\nu+1/2)}{z} f^{(s)}_\nu(z) - \frac{\mathrm{d}f^{(s)}_\nu(z)}{\mathrm{d}z}\\ f^{(s)}_{\nu-1}(z) &= \frac{(\nu-1/2)}{z} f^{(s)}_\nu(z) + \frac{\mathrm{d}f^{(s)}_\nu(z)}{\mathrm{d}z}\end{aligned} \tag{4.1}$$

and the constant can be deduced, without loss of generality, by applying these relations to the Riccati–Hankel function $\zeta^{(1)}_\nu(z)$ in the asymptotic limiting case of $z \to \infty$. Thus, the function simplifies to $\zeta^{(1)}_\nu(z) \to -\mathrm{i}\exp\mathrm{i}\left(z - \gamma^0_\nu\right)$ and the relations become

$$\zeta^{(1)}_{\nu+1}(z) \underset{z\to\infty}{\simeq} -\frac{\mathrm{d}\zeta^{(1)}_\nu(z)}{\mathrm{d}z} = -\mathrm{i}\zeta^{(1)}_\nu(z)$$

$$\zeta^{(1)}_{\nu-1}(z) \underset{z\to\infty}{\simeq} \frac{\mathrm{d}\zeta^{(1)}_\nu(z)}{\mathrm{d}z} = \mathrm{i}\zeta^{(1)}_\nu(z)$$

to give

$$\exp\left(\mathrm{i}\gamma^0_{\nu\pm1}\right) = \pm\mathrm{i}\exp\left(\mathrm{i}\gamma^0_\nu\right).$$

After ℓ recursions,

$$\exp(\mathrm{i}\gamma^0_{\nu\pm\ell}) = (\pm\mathrm{i})^\ell \exp\left(\mathrm{i}\gamma^0_\nu\right)$$

and

$$\gamma^0_{\nu\pm\ell} = \gamma^0_\nu \pm \ell\frac{\pi}{2} \tag{4.2}$$

are obtained. A plot of the phase constant against ν will therefore generate a straight line of gradient $\frac{\pi}{2}$ that passes through the origin at $\nu = 1/2$ in accordance with (3.5*c*). Thus,

$$\gamma^0_\nu = (\nu - 1/2)\frac{\pi}{2}. \tag{4.3}$$

5. Negative orders

Inspection of the differential equation (2.1) indicates that it is invariant when the order is reversed in sign and because of this R–B functions of negative orders are possible solutions of the equation. It then follows that the new solutions may be derived by simply changing the signs of ν in the original solutions. Hence the Riccati–Hankel function $\zeta^{(1)}_\nu(z)$, when written in the form of (A2*c*),

$$\zeta^{(1)}_\nu(z) = -\mathrm{i}\frac{[\varphi_{-\nu}(z) - \mathrm{e}^{-\mathrm{i}\nu\pi}\varphi_\nu(z)]}{\sin\nu\pi}$$

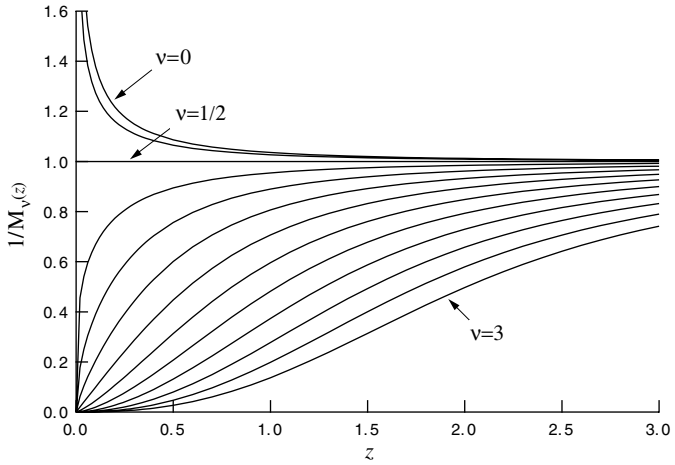

Figure 1. The reciprocal $M_\nu(z)$ function for $\nu = 0$ to 3 in steps of $1/4$.

transforms into

$$\zeta_{-\nu}^{(1)}(z) = \mathrm{i}\frac{[\varphi_\nu(z) - \mathrm{e}^{\mathrm{i}\nu\pi}\varphi_{-\nu}(z)]}{\sin\nu\pi} = \exp(\mathrm{i}\upsilon\pi)\zeta_\nu^{(1)}(z) \tag{5.1}$$

under the operation $\nu \to -\nu$. Similarly,

$$\zeta_\nu^{(1)}(z) = -\mathrm{i}\, M_\nu(z)\exp\mathrm{i}\theta_\nu(z)$$

becomes

$$\zeta_{-\nu}^{(1)}(z) = -\mathrm{i}\, M_{-\nu}(z)\exp\mathrm{i}\theta_{-\nu}(z)$$

and these yield

$$M_{-\nu}(z)\exp\mathrm{i}\theta_{-\nu}(z) = \exp(\mathrm{i}\nu\pi)M_\nu(z)\exp\mathrm{i}\theta_\nu(z) \tag{5.2}$$

on substitution into (5.1). But since the amplitudes $M_\nu(z)$ and $M_{-\nu}(z)$ are both defined as positive functions, the previous equation can be decomposed into

$$M_{-\nu}(z) = M_\nu(z) \tag{5.3a}$$

and

$$\theta_{-\nu}(z) = \theta_\nu(z) + \nu\pi. \tag{5.3b}$$

Also,

$$\gamma_{-\nu}^0 = \gamma_\nu^0 - \nu\pi \qquad \gamma_{-\nu}(z) = \gamma_\nu(z) \tag{5.4}$$

from (3.3a) and (4.3). Further symmetry analysis on the remaining properties shows that $N_\nu(z)$ and $\Delta_\nu(z)$ are even functions of ν and

$$\phi_{-\nu}(z) = \phi_\nu(z) + \nu\pi. \tag{5.5}$$

6. General analysis

The general behaviour of the phase and amplitude functions of the R–B functions is presented in figures 1–3, where the order is incremented between 0 and 3 in steps of $1/4$ and z is varied. All three functions $1/M_\nu(z)$, $\theta_\nu(z)$ and $\gamma_\nu(z)$ are seen to be monotonic and the gradients of

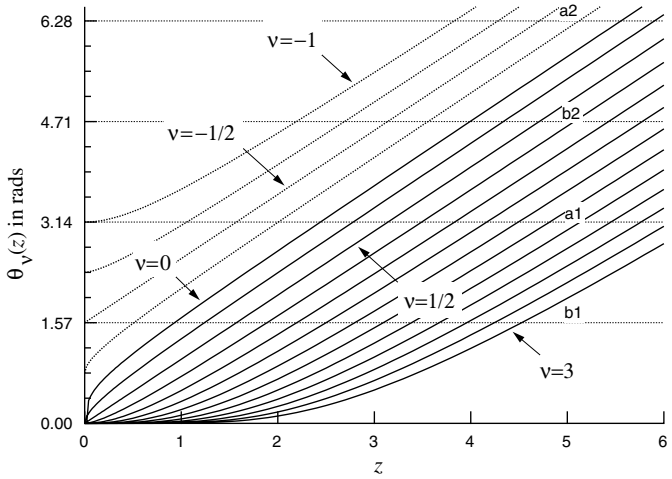

Figure 2. The spatial phase angle $\theta_\nu(z)$ for $\nu = -1$ to 3 in steps of 1/4. Negative orders are included for comparison.

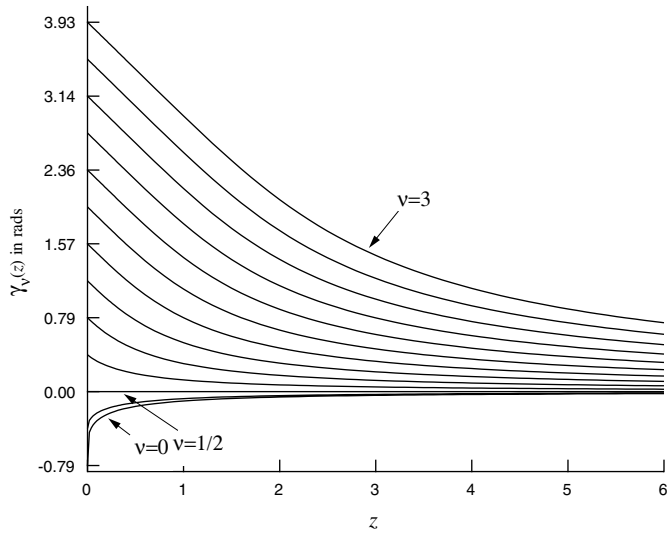

Figure 3. The auxiliary phase $\gamma_\nu(z)$ for $\nu = 0$ to 3 in steps of 1/4.

the two phase angles are simply related to the amplitude by

$$\frac{1}{M_\nu^2(z)} = \theta_\nu'(z) = 1 + \gamma_\nu'(z)$$

through (2.6*b*) and (3.3*a*). As a consequence, the traces for $\nu = 1/2$ are especially simple being straight lines of unit or zero gradient; $M_{1/2}(z) = 1$, $\theta_{1/2}'(z) = 1$ and $\gamma_{1/2}'(z) = 0$. For other orders the functions generate curves that either approach or become parallel to the $\nu = 1/2$ trace in the asymptotic limit. Despite this, the most striking differences in the graphs occur at the origin and lead to a classification according to (a) $0 \leqslant \nu < 1/2$, (b) $\nu = 1/2$ or (c) $\nu > 1/2$ as exemplified in table 1.

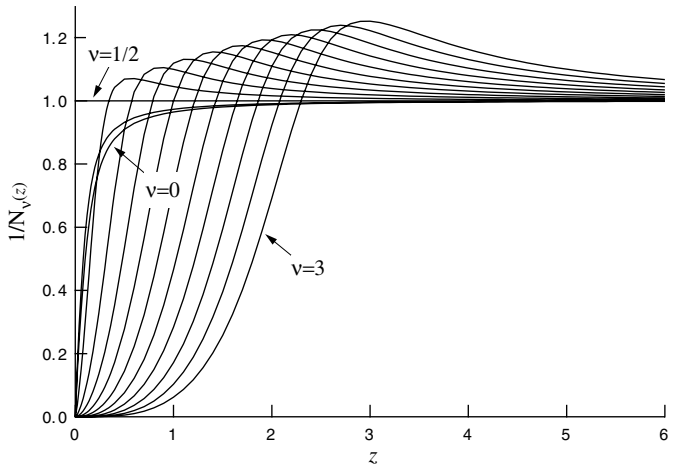

Figure 4. The reciprocal $N_\nu(z)$ function for $\nu = 0$ to 3 in steps of $1/4$.

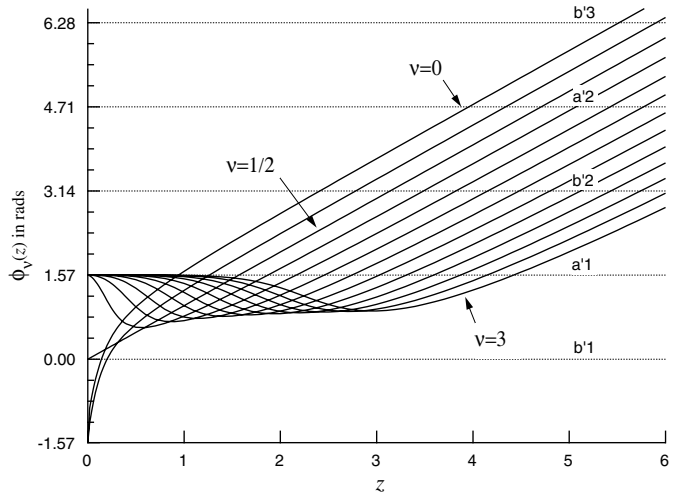

Figure 5. The spatial phase angle $\phi_\nu(z)$ for $\nu = 0$ to 3 in steps of $1/4$.

Table 1. Initial values of the phase and amplitude functions.

Function	$0 \leqslant \nu < 1/2$	$\nu = 1/2$	$\nu > 1/2$
$M_\nu(0)$	0	1	$+\infty$
$\theta_\nu(0)$	0	0	0
$\gamma_\nu(0)$	<0	0	>0
$N_\nu(0)$	$+\infty$	1	$+\infty$
$\phi_\nu(0)$	$-\pi/2$	0	$\pi/2$
$\Delta_\nu(0)$	$-\pi/2$	0	$\pi/2$

In the case of the derivatives of the R–B functions, the properties of interest are $1/N_\nu(z)$, $\phi_\nu(z)$ and $\Delta_\nu(z)$ which are plotted in figures 4–6. Only the last of these is monotonic in z,

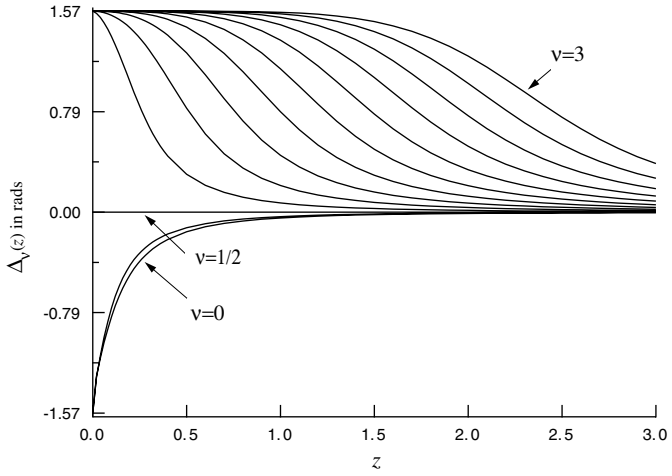

Figure 6. The phase shift $\Delta_\nu(z)$ for $\nu = 0$ to 3 in steps of $1/4$.

as $1/N_\nu(z)$ and $\phi_\nu(z)$ exhibit maxima and minima, respectively, at $z = \sqrt{\mu_1}$ for $\nu > 1/2$ according to (2.7). Initial values of the functions are also included in table 1.

6.1. Near-field analysis

Values of the functions near the origin can be generally found from solutions of (2.1) in the form of ascending series in z,

$$\varphi_{\pm\nu}(z) = \sqrt{\pi}\left[\frac{z}{2}\right]^{\frac{1}{2}\pm\nu} \sum_{p=0}^{\infty} \frac{\left[\frac{-z^2}{4}\right]^p}{p!\Gamma\,(1+p\pm\nu)}, \tag{6.1}$$

by retaining only the dominant terms of $\varphi_\nu(z)$, $\chi_\nu(z)$, $\varphi'_\nu(z)$ and $\chi'_\nu(z)$ as $z \to 0$. This leads to three separate cases of order 0, $1/2$ and υ that need to be considered for the amplitude and phase functions. The R–B functions therefore simplify into

$$\begin{aligned}
&\varphi_0(z) \simeq \sqrt{\frac{\pi z}{2}} && \varphi_{1/2}(z) \simeq z && \varphi_\nu(z) \simeq \frac{\sqrt{\pi}}{\Gamma(1+\nu)}\left[\frac{z}{2}\right]^{\frac{1}{2}+\nu} \\
&\chi_0(z) \simeq \sqrt{\frac{2z}{\pi}}l(z) && \chi_{1/2}(z) \simeq -1+\frac{z^2}{2} && \chi_\nu(z) \simeq -\frac{\Gamma(\nu)}{\sqrt{\pi}}\left[\frac{z}{2}\right]^{\frac{1}{2}-\nu},
\end{aligned} \tag{6.2}$$

where $l(z) = \ln\left(\frac{z}{2}\right) + \gamma$ in which γ is the Euler–Mascheroni constant. Combinations of these also yield

$$\begin{aligned}
&M_0(z) \simeq \sqrt{\frac{2z}{\pi}}\,|l(z)| && M_{1/2}(z) = 1 && M_\nu(z) \simeq \frac{\Gamma(\nu)}{\sqrt{\pi}}\left[\frac{z}{2}\right]^{\frac{1}{2}-\nu} \\
&\theta_0(z) \simeq -\frac{\pi}{2l(z)} && \theta_{1/2}(z) = z && \theta_\nu(z) \simeq \frac{\pi}{\nu\,\Gamma^2(\nu)}\left[\frac{z}{2}\right]^{2\nu} \\
&\gamma_0(z) \simeq -\frac{\pi}{4} - z - \frac{\pi}{2l(z)} && \gamma_{1/2}(z) = 0 && \gamma_\nu(z) \simeq \gamma_\nu^0 - z + \frac{\pi}{\nu\,\Gamma^2(\nu)}\left[\frac{z}{2}\right]^{2\nu},
\end{aligned} \tag{6.3}$$

to show that $\theta_\nu(z) \geqslant 0$, $\theta_\nu(z) \to 0$ in the limit $z \to 0$ for $\nu \geqslant 0$ and $M_\nu(0) = 0$, 1 and ∞ when $0 \leqslant \nu < 1/2$, $\nu = 1/2$ and $\nu > 1/2$, respectively. Expressions for the auxiliary phase

angles were found from (3.3*a*) by

$$\gamma_\nu(z) = \gamma_\nu^0 - z + \theta_\nu(z).$$

Other functions are

$$\begin{aligned}
&N_0(z) \simeq \frac{1}{\sqrt{2\pi z}}|l(z)+2| && N_{1/2}(z) = 1 && N_\nu(z) \simeq |2\nu-1|\frac{\Gamma(\nu)}{4\sqrt{\pi}}\left[\frac{z}{2}\right]^{-\frac{1}{2}-\nu}\\
&\phi_0(z) \simeq -\frac{\pi}{2} - \frac{\pi}{2\,[l(z)+2]} && \phi_{1/2}(z) = z && \phi_\nu(z) \simeq \pm\frac{\pi}{2} - \left(\frac{2\nu+1}{2\nu-1}\right)\theta_\nu(z)\\
&\Delta_0(z) \simeq -\frac{\pi}{2} + \frac{\pi}{l(z)\,[l(z)+2]} && \Delta_{1/2}(z) = 0 && \Delta_\nu(z) \simeq \pm\frac{\pi}{2} - \left(\frac{4\nu}{2\nu-1}\right)\theta_\nu(z).
\end{aligned} \tag{6.4}$$

Here the upper (lower) signs of $\frac{\pi}{2}$ apply to orders greater (less) than $1/2$ and are associated with signs of $\tan\phi_\nu(z)$ and $\tan\Delta_\nu(z)$ in

$$\tan\Delta_\nu(z) \simeq \frac{(2\nu+1)}{4\nu}\tan\phi_\nu(z) \simeq \frac{(2\nu-1)}{4\nu\,\theta_\nu(z)}. \tag{6.5}$$

All the values listed in table 1 can accordingly be explained.

6.2. *Far-field analysis*

In the far field, when ν is fixed and $z \to \infty$ (2.1) has solutions that contain asymptotic series

$$\begin{aligned}
\zeta_\nu^{(1)}(z) &= -\mathrm{i}\,[P_\nu(z) + \mathrm{i}Q_\nu(z)]\exp\mathrm{i}\big(z-\gamma_\nu^0\big)\\
\zeta_\nu^{(2)}(z) &= \mathrm{i}\,[P_\nu(z) - \mathrm{i}Q_\nu(z)]\exp-\mathrm{i}\big(z-\gamma_\nu^0\big),
\end{aligned} \tag{6.6}$$

where

$$\begin{aligned}
P_\nu(z) &= 1 - \frac{\mu_1\mu_2}{2!(2z)^2} + \frac{\mu_1\mu_2\mu_3\mu_4}{4!(2z)^4} - \cdots\\
Q_\nu(z) &= \frac{\mu_1}{1!(2z)} - \frac{\mu_1\mu_2\mu_3}{3!(2z)^3} + \frac{\mu_1\mu_2\mu_3\mu_4\mu_5}{5!(2z)^5} - \cdots
\end{aligned} \tag{6.7}$$

in which $\mu_0 = 1$ and $\mu_S = \nu^2 - (s-1/2)^2$. A comparison of (2.2*c*) and (2.2*d*) with (6.6) then yields

$$P_\nu(z) \pm \mathrm{i}Q_\nu(z) = M_\nu(z)\exp\left[\pm\mathrm{i}\gamma_\nu(z)\right] \tag{6.8a}$$

and allows the amplitude and auxiliary phase to be defined by

$$\begin{aligned}
M_\nu^2(z) &= P_\nu^2(z) + Q_\nu^2(z)\\
&= 1 + \frac{1}{2}\frac{\mu_1}{z^2} + \frac{1.3}{2.4}\frac{\mu_1\mu_2}{z^4} + \frac{1.3.5}{2.4.6}\frac{\mu_1\mu_2\mu_3}{z^6} + \cdots
\end{aligned} \tag{6.8b}$$

$$\gamma_\nu(z) = \tan^{-1}\left[\frac{Q_\nu(z)}{P_\nu(z)}\right], \tag{6.8c}$$

where the branch of $\gamma_\nu(z)$ is fixed by the condition $\gamma_\nu(0) = \gamma_\nu^0$. Also,

$$\begin{aligned}
\tan\Delta_\nu(z) &= -\frac{1}{2}\left[M_\nu^2(z)\right]'\\
&= \frac{1}{2}\frac{\mu_1}{z^3}\left[1 + \frac{3}{2}\frac{\mu_2}{z^2} + \frac{3.5}{2.4}\frac{\mu_2\mu_3}{z^4} + \cdots\right].
\end{aligned} \tag{6.9}$$

Table 2. Initial values of R–B functions.

Function	$0 \leqslant \nu < 1/2$	$\nu = 1/2$	$\nu > 1/2$
$\varphi_\nu(0)$	0	0	0
$\chi_\nu(0)$	0	-1	$-\infty$
$\varphi'_\nu(0)$	$+\infty$	1	0
$\chi'_\nu(0)$	$-\infty$	0	$+\infty$

Limiting forms of the functions as $z \to \infty$ are

$$\begin{aligned} \theta_\nu(z) &\simeq z - \gamma_\nu^0 + \frac{\mu_1}{2z} & [M_\nu(z)]^{-1} &\simeq 1 - \frac{\mu_1}{4z^2} \\ \phi_\nu(z) &\simeq z - \gamma_\nu^0 + \frac{\mu_1}{2z} & [N_\nu(z)]^{-1} &\simeq 1 + \frac{\mu_1}{4z^2} \\ \Delta_\nu(z) &\simeq \frac{\mu_1}{2z^3} & \gamma_\nu(z) &\simeq \frac{\mu_1}{2z}. \end{aligned} \tag{6.10}$$

The sign of μ_1,which is negative for $0 \leqslant \nu < 1/2$ or positive when $\nu > 1/2$, then determines whether a function in figures 1–6 approaches its limiting value from below or above. Furthermore by extrapolating the asymptotes of $\theta_\nu(z)$ and $\phi_\nu(z)$, the intercepts on the vertical axes are

$$-\gamma_\nu^0 = -(\nu - 1/2)\frac{\pi}{2}.$$

7. Zeros of R–B Functions

The determination of the locations of the zeros of R–B functions requires different considerations depending on whether these are at or away from the origin. In the former case, it has been shown in table 1 that the amplitude factors can have values of 0, 1 or ∞ while the phase angles may be $-\pi/2$, 0 or $\pi/2$. Thus to find which of the R–B functions have null values, we return to the simplified expressions of (6.2) to obtain table 2.

Away from the origin, the amplitude functions $M_\nu(z)$and $N_\nu(z)$ are both finite and nonzero and so R–B functions will be zero only when the phase angles $\theta_\nu(z)$ or $\phi_\nu(z)$ are integer multiples of $\pi/2$. Four conditions are therefore of interest and these are displayed as horizontal lines labelled as, bs in figure 2 and a′s, b′s in figure 5. The locations of the zeros $\alpha_{\nu,s}$, $\beta_{\nu,s}$ of $\varphi_\nu(z)$, $\chi_\nu(z)$ and $\alpha'_{\nu,s}$, $\beta'_{\nu,s}$ of $\varphi'_\nu(z)$, $\chi'_\nu(z)$ are then found from where the lines intersect the respective traces. Computed values of the zeros in radians (upper) and relative values in units of $\pi/2$ (lower) are given in tables 3 and 4. But in the case of $\beta'_{\nu,1}$, figure 5 shows there is no intersection with the line $b'1$ when $\nu > 1/2$ and N.S. is entered in table 4 to indicate no solution. Expressions for the associated R–B functions at the zeros, where $s = 1, 2, 3, \ldots$, are

Case A : $\theta_\nu(\alpha_{\nu,s}) = s\pi$

$$\begin{aligned} \varphi_\nu(\alpha_{\nu,s}) &= 0 & \chi_\nu(\alpha_{\nu,s}) &= (-1)^{s-1} M_\nu(\alpha_{\nu,s}) \\ \varphi'_\nu(\alpha_{\nu,s}) &= \frac{(-1)^s}{M_\nu(\alpha_{\nu,s})} & \chi'_\nu(\alpha_{\nu,s}) &= \frac{(-1)^s \tan\Delta_\nu(\alpha_{\nu,s})}{M_\nu(\alpha_{\nu,s})}. \end{aligned} \tag{7.1a}$$

Case B : $\theta_\nu(\beta_{\nu,s}) = (2s-1)\frac{\pi}{2}$

$$\begin{aligned} \varphi_\nu(\beta_{\nu,s}) &= (-1)^{s-1} M_\nu(\beta_{\nu,s}) & \chi_\nu(\beta_{\nu,s}) &= 0 \\ \varphi'_\nu(\beta_{\nu,s}) &= \frac{(-1)^s \tan\Delta_\nu(\beta_{\nu,s})}{M_\nu(\beta_{\nu,s})} & \chi'_\nu(\beta_{\nu,s}) &= \frac{(-1)^{s-1}}{M_\nu(\beta_{\nu,s})}. \end{aligned} \tag{7.1b}$$

Table 3. Zeros of $\varphi_\nu(z)$ and $\chi_\nu(z)$ in radians (upper) and units of $\pi/2$ (lower).

ν	$\beta_{\nu,1}$	$\alpha_{\nu,1}$	$\beta_{\nu,2}$	$\alpha_{\nu,2}$	$\beta_{\nu,3}$	$\alpha_{\nu,3}$
0	0.8936	2.4048	3.9577	5.5201	7.0861	8.6537
	0.5689	1.5309	2.5196	3.5142	4.5112	5.5091
1/4	1.2417	2.7809	4.3408	5.9061	7.4737	9.0424
	0.7905	1.7704	2.7634	3.7599	4.7579	5.7566
1/2	1.5708	3.1416	4.7124	6.2832	7.8540	9.4248
	1.0000	2.0000	3.0000	4.0000	5.0000	6.0000
3/4	1.8881	3.4910	5.0748	6.6526	8.2278	9.8016
	1.2020	2.2224	3.2307	4.2352	5.2380	6.2399
1	2.1971	3.8317	5.4297	7.0156	8.5960	10.173
	1.3987	2.4393	3.4567	4.4663	5.4724	6.4767
5/4	2.5001	4.1654	5.7782	7.3729	8.9592	10.541
	1.5916	2.6518	3.6785	4.6937	5.7036	6.7105
3/2	2.7984	4.4934	6.1213	7.7253	9.3179	10.904
	1.7815	2.8606	3.8969	4.9181	5.9320	6.9418
7/4	3.0929	4.8166	6.4596	8.0732	9.6725	11.264
	1.9690	3.0663	4.1123	5.1396	6.1577	7.1707
2	3.3842	5.1356	6.7938	8.4172	10.023	11.620
	2.1544	3.2694	4.3251	5.3586	6.3812	7.3974
9/4	3.6730	5.4511	7.1243	8.7577	10.371	11.973
	2.3383	3.4703	4.5355	5.5753	6.6024	7.6221
5/2	3.9595	5.7635	7.4516	9.0950	10.716	12.323
	2.5207	3.6692	4.7438	5.7901	6.8218	7.8450
11/4	4.2441	6.0730	7.7759	9.4294	11.057	12.670
	2.7019	3.8662	4.9503	6.0029	7.0394	8.0662
3	4.5270	6.3802	8.0976	9.7610	11.396	13.015
	2.8820	4.0618	5.1551	6.2140	7.2552	8.2857

Case C : $\phi_\nu(\alpha'_{\nu,s}) = (2s-1)\,\frac{\pi}{2}$

$$\begin{aligned} \varphi_\nu(\alpha'_{\nu,s}) &= \frac{(-1)^{s-1}}{N_\nu(\alpha'_{\nu,s})} & \chi_\nu(\alpha'_{\nu,s}) &= \frac{(-1)^s \tan\Delta_\nu(\alpha'_{\nu,s})}{N_\nu(\alpha'_{\nu,s})} \\ \varphi'_\nu(\alpha'_{\nu,s}) &= 0 & \chi'_\nu(\alpha'_{\nu,s}) &= (-1)^{s-1} N_\nu(\alpha'_{\nu,s}). \end{aligned} \tag{7.1c}$$

Case D : $\phi_\nu(\beta'_{\nu,s}) = (s-1)\,\pi$

$$\begin{aligned} \varphi_\nu(\beta'_{\nu,s}) &= \frac{(-1)^s \tan\Delta_\nu(\beta'_{\nu,s})}{N_\nu(\beta'_{\nu,s})} & \chi_\nu(\beta'_{\nu,s}) &= \frac{(-1)^s}{N_\nu(\beta'_{\nu,s})} \\ \varphi'_\nu(\beta'_{\nu,s}) &= (-1)^{s-1} N_\nu(\beta'_{\nu,s}) & \chi'_\nu(\beta'_{\nu,s}) &= 0. \end{aligned} \tag{7.1d}$$

An alternative procedure for finding the zeros is illustrated in figures 7 and 8 for $\nu = 0$, 2 and 4. Using (3.3), the relations for $\theta_\nu(\alpha_{\nu,s})$, $\theta_\nu(\beta_{\nu,s})$, $\phi_\nu(\alpha'_{\nu,s})$ and $\phi_\nu(\beta'_{\nu,s})$ above are converted into

$$\gamma_\nu(\alpha_{\nu,s}) = (2s+\nu-1/2)\,\frac{\pi}{2} - \alpha_{\nu,s} \tag{7.2a}$$

$$\gamma_\nu(\beta_{\nu,s}) = (2s+\nu-3/2)\,\frac{\pi}{2} - \beta_{\nu,s} \tag{7.2b}$$

$$\gamma_\nu(\alpha'_{\nu,s}) + \Delta_\nu(\alpha'_{\nu,s}) = (2s+\nu-3/2)\,\frac{\pi}{2} - \alpha'_{\nu,s} \tag{7.2c}$$

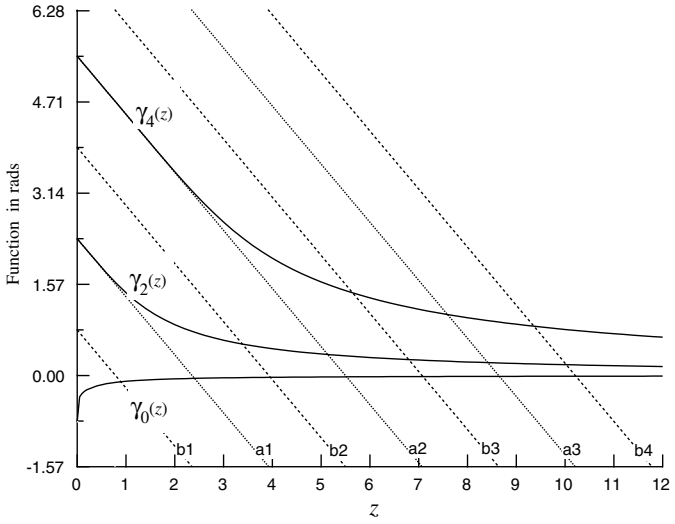

Figure 7. Graphical determination of zeros of $\varphi_\nu(z)$ and $\chi_\nu(z)$ for $\nu = 0, 2$ and 4.

Table 4. Zeros of $\varphi'_\nu(z)$ and $\chi'_\nu(z)$ in radians (upper) and units of $\pi/2$ (lower). N.S. indicates no solution exists.

ν	$\beta'_{\nu,1}$	$\alpha'_{\nu,1}$	$\beta'_{\nu,2}$	$\alpha'_{\nu,2}$	$\beta'_{\nu,3}$	$\alpha'_{\nu,3}$
0	0.1421	0.9408	2.4110	3.9594	5.5208	7.0864
	0.0905	0.5989	1.5349	2.5206	3.5148	4.5114
1/4	0.2001	1.2624	2.7841	4.3418	5.9066	7.4739
	0.1274	0.8037	1.7724	2.7641	3.7602	4.7581
1/2	0.0000	1.5708	3.1416	4.7124	6.2832	7.8540
	0.0000	1.0000	2.0000	3.0000	4.0000	5.0000
3/4	N.S.	1.8711	3.4878	5.0737	6.6521	8.2275
		1.1912	2.2204	3.2299	4.2348	5.2378
1	N.S.	2.1659	3.8255	5.4274	7.0145	8.5954
		1.3789	2.4354	3.4553	4.4656	5.4721
5/4	N.S.	2.4564	4.1564	5.7748	7.3713	8.9583
		1.5638	2.6460	3.6765	4.6928	5.7032
3/2	N.S.	2.7437	4.4817	6.1168	7.7230	9.3166
		1.7467	2.8531	3.8942	4.9166	5.9311
7/4	N.S.	3.0283	4.8025	6.4540	8.0704	9.6709
		1.9279	3.0574	4.1087	5.1378	6.1568
2	N.S.	3.3108	5.1192	6.7872	8.4139	10.022
		2.1077	3.2589	4.3207	5.3565	6.3802
9/4	N.S.	3.5913	5.4326	7.1168	8.7538	10.369
		2.2863	3.4584	4.5308	5.5730	6.6011
5/2	N.S.	3.8702	5.7429	7.4431	9.0906	10.713
		2.4638	3.6561	4.7384	5.7872	6.8201
11/4	N.S.	4.1478	6.0506	7.7665	9.4244	11.054
		2.6406	3.8519	4.9443	5.9998	7.0372
3	N.S.	4.4241	6.3559	8.0872	9.7555	11.393
		2.8165	4.0464	5.1483	6.2105	7.2530

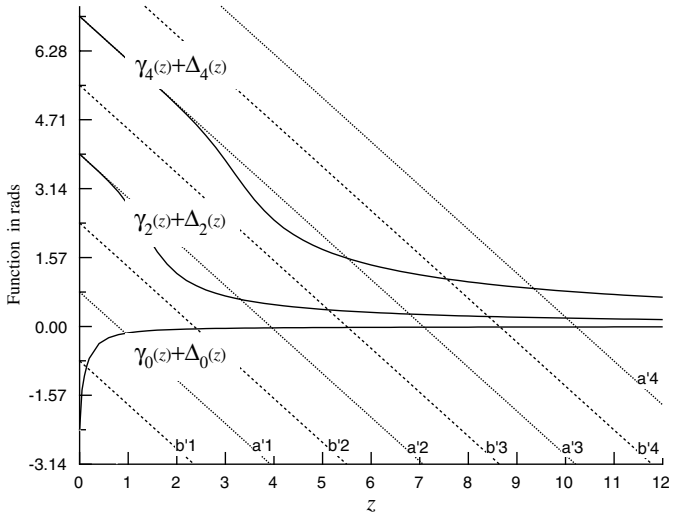

Figure 8. Graphical determination of zeros of $\varphi'_\nu(z)$ and $\chi'_\nu(z)$ for $\nu = 0$, 2 and 4.

$$\gamma_\nu(\beta'_{\nu,s}) + \Delta_\nu(\beta'_{\nu,s}) = (2s + \nu - 5/2)\,\frac{\pi}{2} - \beta'_{\nu,s}. \tag{7.2d}$$

However all four of these relations are invariant under the joint operations of $s \to s - p$ and $\nu \to \nu + 2p$ when p is an integer. As a consequence, the lines labelled a3 and b3 in figure 7 intersect the plots of $\gamma_0(z)$, $\gamma_2(z)$ and $\gamma_4(z)$ to give the zeros $\alpha_{0,3} = 8.6537(5.5091)$, $\alpha_{2,2} = 8.4172\,(5.3586)$, $\alpha_{4,1} = 7.5883\,(4.8309)$ and $\beta_{0,3} = 7.0861\,(4.5112)$, $\beta_{2,2} = 6.7938\,(4.1123)$, $\beta_{4,1} = 5.6452\,(3.5938)$, respectively, where the first of the values is in radians and the second in units of $\pi/2$. Similarly lines a4and b4 each intersect the plots $\gamma_0(z)$, $\gamma_2(z)$, $\gamma_4(z)$ and $\gamma_6(z)$ to yield more zeros. The same strategy can be applied to figure 8 to find the zeros of $\varphi'_\nu(z)$ and $\chi'_\nu(z)$ but the intersects are now with the combined function $\gamma_\nu(z) + \Delta_\nu(z)$. It is clear from figures 7 and 8 that the crossing points converge rapidly with increasing s to give the limiting expressions:

$$\begin{aligned} \alpha_{\nu,s} &\underset{s\to\infty}{\simeq} (2s + \nu - 1/2)\frac{\pi}{2}, \qquad & \beta_{\nu,s} &\underset{s\to\infty}{\simeq} (2s + \nu - 3/2)\frac{\pi}{2}, \\ \alpha'_{\nu,s} &\underset{s\to\infty}{\simeq} (2s + \nu - 3/2)\frac{\pi}{2}, \qquad & \beta'_{\nu,s} &\underset{s\to\infty}{\simeq} (2s + \nu - 5/2)\frac{\pi}{2}. \end{aligned} \tag{7.3}$$

For example, the zeros $\beta_{0,4} = 10.2223\,(6.5077)$, $\beta_{2,3} = 10.0235\,(6.3811)$, $\beta_{4,2} = 9.3616\,(5.9598)$ and $\alpha'_{0,4} = 10.2225\,(6.5078)$, $\alpha'_{2,3} = 10.0215\,(6.3799)$, $\alpha'_{4,2} = 9.3481\,(5.9512)$ should be compared with the limit value of $10.2102\,(6.5000)$.

8. Discussion

The solutions of the R–B differential equation when z is real have been examined in detail and it is shown that an R–B function can be usefully represented in terms of an amplitude function $M_\nu(z)$ and a spatial phase function $\theta_\nu(z)$. Indeed, the phase angle is a common property of all Bessel functions since (3.2) can be simply extended to cover cylindrical and spherical waves through

$$\theta_\nu(z) = \tan^{-1}\left[-\frac{\varphi_\nu(z)}{\chi_\nu(z)}\right] = \tan^{-1}\left[-\frac{J_\nu(z)}{Y_\nu(z)}\right] \tag{8.1a}$$

and

$$\lim_{z\to 0}\frac{\varphi_\nu(z)}{\chi_\nu(z)}=\lim_{z\to 0}\frac{J_\nu(z)}{Y_\nu(z)}=0, \tag{8.1b}$$

subject to the initial phase condition

$$\theta_\nu(0)=0; \qquad 0\leqslant \nu. \tag{8.1c}$$

Thus, cylindrical Bessel and spherical Bessel functions can be written as

$$J_\ell(z)=\sqrt{\frac{2}{\pi z}}\varphi_\ell(z)=\sqrt{\frac{2}{\pi z}}M_\ell(z)\sin\theta_\ell(z) \tag{8.2a}$$

$$Y_\ell(z)=\sqrt{\frac{2}{\pi z}}\chi_\ell(z)=-\sqrt{\frac{2}{\pi z}}M_\ell(z)\cos\theta_\ell(z) \tag{8.2b}$$

and

$$j_\ell(z)=\frac{1}{z}\varphi_{\ell+1/2}(z)=\frac{1}{z}M_{\ell+1/2}(z)\sin\theta_{\ell+1/2}(z) \tag{8.2c}$$

$$y_\ell(z)=\frac{1}{z}\chi_{\ell+1/2}(z)=-\frac{1}{z}M_{\ell+1/2}(z)\cos\theta_{\ell+1/2}(z), \tag{8.2d}$$

where $\ell=0,1,2,\ldots$. It should be noted that at the origin, $\varphi_\nu(z)$ is equal to zero for all non-negative orders while the Bessel functions $J_0(0)=j_0(0)=1$ but $J_\ell(0)=j_\ell(0)=0$ for $\ell>0$. This contrasts with $\chi_\nu(z)$ which can be equal to zero when $0\leqslant\nu<1/2$, -1 for $\nu=1/2$ and is singular when $1/2<\nu<\infty$ whereas $Y_\ell(z)$, $y_\ell(z)$ are always singular at the origin.

All three Bessel function have a phase angle

$$\theta_\nu(z)=z-\gamma_\nu^0+\gamma_\nu(z), \tag{8.3}$$

in which the phase constant is $\gamma_\nu^0=(\nu-1/2)\frac{\pi}{2}$ and the auxiliary phase angle $\gamma_\nu(z)$ is a monotonic function of z such that $\gamma_\nu(0)=\gamma_\nu^0$, $\gamma_\nu(z)\underset{z\to\infty}{\simeq}\tan^{-1}\left[\frac{Q_\nu(z)}{P_\nu(z)}\right]$ with $\lim_{z\to\infty}\gamma_\nu(z)=0$. Moreover, when $\nu=\ell+1/2$,

$$\gamma_{\ell+1/2}(z)=\tan^{-1}\left[\frac{Q_{\ell+1/2}(z)}{P_{\ell+1/2}(z)}\right] \tag{8.4}$$

is an exact relation over the complete range $0\leqslant z<\infty$ provided that the branch of the auxiliary phase angle is specified as that for which $\gamma_{\ell+1/2}(0)=\ell\frac{\pi}{2}$. Figures 2 and 3 illustrate the monotonic variation of $\theta_\nu(z)$ and $\gamma_\nu(z)$ with z, and exhibit an ordering of the functions in which: $\theta_{\nu-\delta}(z)>\theta_\nu(z)>\theta_{\nu+\delta}(z)$ and $\gamma_{\nu-\delta}(z)<\gamma_\nu(z)<\gamma_{\nu+\delta}(z)$ for δ positive. It also follows that the zeros of $\varphi_\nu(z)$ and $\chi_\nu(z)$ will be ordered according to $\alpha_{\nu-\delta,s}<\alpha_{\nu,s}<\alpha_{\nu+\delta,s}$ and $\beta_{\nu-\delta,s}<\beta_{\nu,s}<\beta_{\nu+\delta,s}$. Furthermore, the zeros of $\varphi_\nu(z)$, $\chi_\nu(z)$ in table 3 agree with the listed values of the zeros of cylindrical Bessel functions $J_\nu(z)$, $Y_\nu(z)$ for $\upsilon=0,1,2,3$ and spherical Bessel functions $j_\ell(z)$, $y_\ell(z)$ when $\ell=\upsilon-1/2$, $\upsilon=1/2,3/2,5/2$.

A few plots of negative order, computed by (5.3*b*), are included in figure 2 for comparison. However, more importantly, the graph displays the locations of the various zeros of $\varphi_\nu(z)$ and $\chi_\nu(z)$ and it may be used to examine the general properties and relations associated with the zeros of Bessel functions. Some examples are given below.

(a) The zeros of Bessel functions of real order $\nu\geqslant 0$ are limited by the inequalities

$$\alpha_{0,s}(z)\leqslant\alpha_{\nu,s}(z) \tag{8.5a}$$

and

$$\beta_{0,s}(z) \leqslant \beta_{\nu,s}(z), \tag{8.5b}$$

where $s = 1, 2, 3, \ldots$.

(b) The plots of $\nu = 1/2$ and $\nu = -1/2$ are parallel lines of unit gradient in which the former passes through the origin and the latter has an intercept of $\pi/2$ with the vertical axis. Thus, for $-1/2 \leqslant \nu \leqslant 1/2$, the zeros of $\varphi_\nu(z)$ satisfy the relation

$$(2s + \nu - 1/2)\frac{\pi}{2} \leqslant \alpha_{\nu,s} \leqslant s\pi, \tag{8.6a}$$

which is equivalent to that of [10]. Similarly, for $\chi_\nu(z)$ the zeros are in the range

$$(2s + \nu - 3/2)\frac{\pi}{2} \leqslant \beta_{\nu,s} \leqslant (2s - 1)\frac{\pi}{2}. \tag{8.6b}$$

(c) Flajolet and Schott [11] showed that the equation $J_\nu(2) = 0$ has no positive zeros. But it is immediately clear from figure 1 that no positive zeros exist for $J_\nu(z)$ below $z = \alpha_{0,1} = 2.4048$ and for $Y_\nu(z)$ below $z = \beta_{0,1} = 0.8936$.

(d) It is possible for Bessel functions of fixed argument and $\nu \geqslant 0$ to have none, one or multiple zeros and indeed common pairs of zeros have been previously computed [12, 13] or investigated using a functional-analytic approach [14]. Nevertheless, we can see directly from the graph that when $\nu \geqslant 0$ there are n multiple zeros of $\varphi_\nu(z)$ and $\chi_\nu(z)$ for a fixed value of z in the ranges $\alpha_{0,n} \leqslant z < \alpha_{0,n+1}$ and $\beta_{0,n} \leqslant z < \beta_{0,n+1}$, respectively, where $\alpha_{0,0} = \beta_{0,0} = 0$ for $n = 0$. Thus for $\varphi_\nu(z)$ or $\chi_\nu(z)$ there are no positive zeros within the ranges $0 \leqslant z < 2.4048$ or $0 \leqslant z < 0.8936$, only single zeros within $2.4048 \leqslant z < 5.5201$ or $0.8936 \leqslant z < 3.9577$ and pairs of zeros in the ranges $5.5201 \leqslant z < 8.6537$ or $3.9577 \leqslant z < 7.0861$. At $z = 5.5201$, one of the zeros will be $\alpha_{0,2}$ situated on the a2 line and the other zero is obtained by dropping a vertical line from $\alpha_{0,2}$ to intersect the a1 line at $\nu = 2.3050$ so as to give $\alpha_{2.3050,1}$ as the second zero. A similar process, involving the b2 and b1 lines, can be followed for $\chi_\nu(z)$ and gives the first pair of zeros as $\beta_{0,2}$ and $\beta_{2.4984,1}$ at $z = 3.9577$.

From figure 1 and table 1 the amplitude function $M_\nu(z)$ is seen to be a monotonic function of z that approaches the plane wave value of $M_\nu(z) \underset{z\to\infty}{\simeq} 1$ in the far field. Nevertheless in the near field, completely different behaviour is exhibited by $M_\nu(z)$ depending on the order being less than, equal to or greater than $1/2$. This can be explained by examining the values of $\varphi_\nu(z)$ and $\chi_\nu(z)$ at the origin:

$$\begin{array}{llll} 0 \leqslant \nu < 1/2 & \varphi_\nu(0) = 0 & \chi_\nu(0) = 0 & M_\nu(0) = 0 \\ \nu = 1/2 & \varphi_\nu(0) = 0 & \chi_\nu(0) = -1 & M_\nu(0) = 1 \\ 1/2 < \nu < \infty & \varphi_\nu(0) = 0 & \chi_\nu(0) = -\infty & M_\nu(0) = +\infty. \end{array}$$

Plots of $\varphi_\nu(z)$ and $\chi_\nu(z)$ intrinsic waveforms for $\nu = 0$ to 2 in steps of $1/2$ are presented in figures 9 and 10. These illustrate the following features:

(a) the zeros, $\alpha_{\nu,s}$ and $\beta_{\nu,s}$, of the functions where the curves cross the z-axis,

(b) maxima and minima at the positions of $\alpha'_{\nu,s}$ and $\beta'_{\nu,s}$ when the first derivatives of the functions are zero and

(c) points of inflexion when the second derivatives of the functions are zero.

Hence $\alpha_{\nu,s}$ and $\beta_{\nu,s}$ are general points of inflexion but for each trace $\nu > 1/2$, a further special point of inflexion is present at $z = \sqrt{\mu_1}$. This is indicated by P_1, $\mathrm{P}_{3/2}$ and P_2 at $z = 0.8860$, 1.4142 and 1.9365 for $\nu = 1$, $3/2$ and 2. It is moreover clear from figure 10, why minima of $\chi_\nu(z)$ are present at $\beta'_{0,1}$ and $\beta'_{1/2,1}$ but absent for $\nu > 1/2$.

A physical explanation of phase constant can now be given. All the plots in figure 9, with the exception of $\nu = 1/2$ which will be used as a reference, require some range of z in

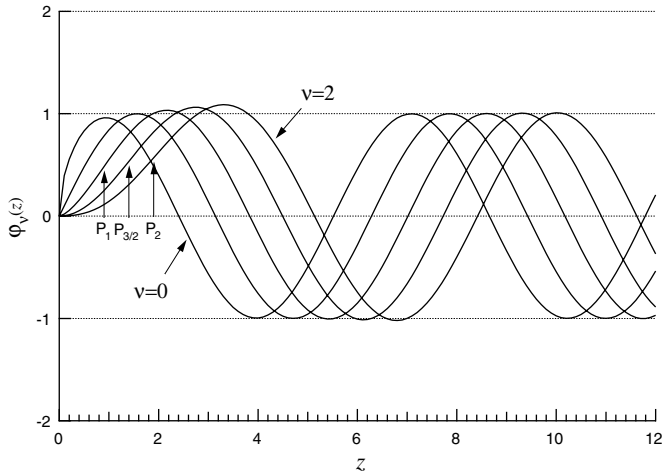

Figure 9. The $\varphi_\nu(z)$ intrinsic waveform for $\nu = 0$ to 2 in steps of $1/2$. $P_1, P_{3/2}$ and P_2 are the positions of special points of inflexion when $\upsilon = 1, 3/2$ and 2.

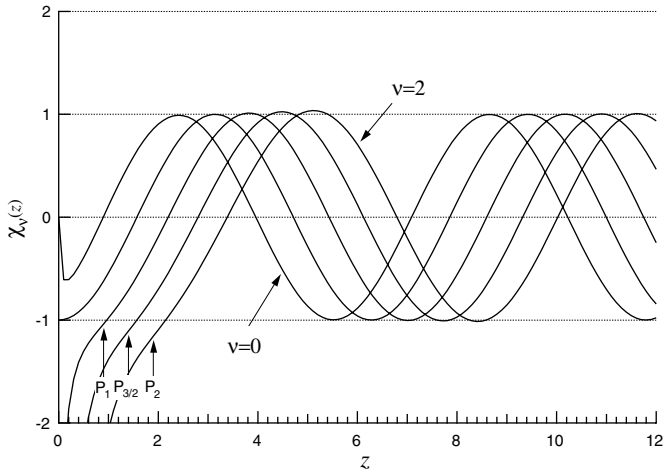

Figure 10. The $\chi_\nu(z)$ intrinsic waveform for $\nu = 0$ to 2 in steps of $1/2$. $P_1, P_{3/2}$ and P_2 are the positions of special points of inflexion when $\upsilon = 1, 3/2$ and 2.

which to adjust from an initial rate of phase change $\theta'_\nu(0) \neq 1$ to the far-field rate of unity. Over this range there will then be an accumulation of a total phase gain for $0 \leqslant \nu < 1/2$ or loss when $\nu > 1/2$ of $-\gamma_\nu^0$ compared with the reference wave. Accordingly, the inclusion of the phase constant in the $\nu = 1/2$ wave will bring it into phase with the far-field behaviour of $\varphi_\nu(z)$:

$$\varphi_\nu(z) \underset{z\to\infty}{\to} \sin\left(z - \gamma_\nu^0\right).$$

Figures 11 and 12 are graphs of $\varphi'_\nu(z)$ and $\chi'_\nu(z)$ intrinsic waveforms for $\nu = 0$ to 2 in steps of $1/2$. These show that the maxima and minima of $\varphi_\nu(z)$ and $\chi_\nu(z)$ become the zeros $\alpha'_{\nu,s}$ and $\beta'_{\nu,s}$, and the original points of inflexion $P_1, P_{3/2}$ and P_2 have been converted into maxima

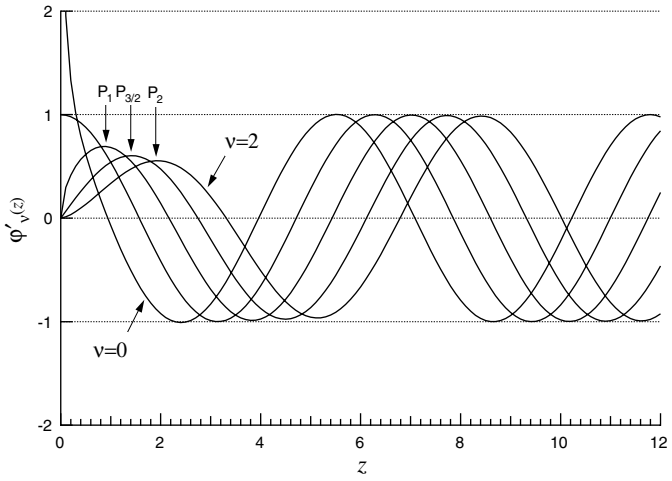

Figure 11. The $\varphi'_\nu(z)$ intrinsic waveform for $\nu = 0$ to 2 in steps of $1/2$.

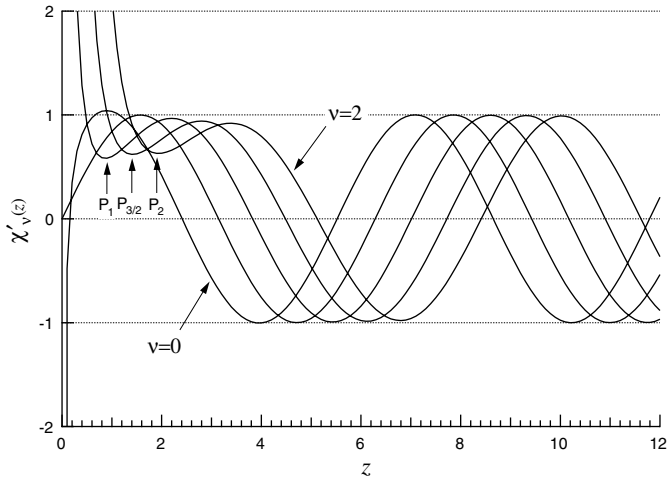

Figure 12. The $\chi'_\nu(z)$ intrinsic waveform for $\nu = 0$ to 2 in steps of $1/2$.

and minima, respectively. The missing minima of figure 10 are therefore responsible for the absence of solutions of $\beta'_{\nu,1}$ in table 4 for $\nu > 1/2$.

Comparing $\varphi_\nu(z)$ with $\chi'_\nu(z)$ in the near field again leads to a distinction among the three ranges of order. This indicates that $\phi_\nu(z) < \theta_\nu(z)$; $0 \leqslant \nu < 1/2$, $\phi_\nu(z) = \theta_\nu(z)$; $\nu = 1/2$ and $\phi_\nu(z) > \theta_\nu(z)$; $1/2 < \nu$, since close to the origin $\chi'_\nu(z)$ jumps between negative, zero and positive values with increasing order. Nonetheless in the far field

$$\varphi_\nu(z) \simeq \chi'_\nu(z) \underset{z\to\infty}{\to} \sin\left(z - \gamma_\nu^0\right)$$

and

$$\varphi'_\nu(z) \simeq -\chi_\nu(z) \underset{z\to\infty}{\to} \cos\left(z - \gamma_\nu^0\right).$$

Appendix. Properties of Riccati–Bessel functions

A.1. Definitions

(a) Differential R–B equation for general function $f_\nu^{(s)}(z)$

$$\left(\frac{\mathrm{d}^2}{\mathrm{d}z^2} + 1 - \frac{\mu_1}{z^2}\right) f_\nu^{(s)}(z) = 0, \qquad \nu = \ell + \delta \qquad \text{for} \quad -1/2 < \delta \leqslant 1/2$$
$$\text{and} \quad \ell = 0, \pm 1, \pm 2, \ldots, \tag{A1}$$

where $\mu_1 = \nu^2 - 1/4$ and s is a label 1– 4 specifying the kind of solution.

(b) Solutions for non-integer order, $\delta \neq 0$

$$f_\nu^{(1)}(z) = \varphi_\nu(z) \tag{A2a}$$

$$f_\nu^{(2)}(z) = \chi_\nu(z) = \frac{[\cos \nu\pi \ \varphi_\nu(z) - \varphi_{-\nu}(z)]}{\sin \nu\pi} \tag{A2b}$$

$$f_\nu^{(3)}(z) = \zeta_\nu^{(1)}(z) = -\mathrm{i}\frac{[\varphi_{-\nu}(z) - \mathrm{e}^{-\mathrm{i}\nu\pi}\varphi_\nu(z)]}{\sin \nu\pi} \tag{A2c}$$

$$f_\nu^{(4)}(z) = \zeta_\nu^{(2)}(z) = \mathrm{i}\frac{[\varphi_{-\nu}(z) - \mathrm{e}^{\mathrm{i}\nu\pi}\varphi_\nu(z)]}{\sin \nu\pi}. \tag{A2d}$$

(c) Solutions for integer order, $\delta = 0$

$$f_\ell^{(1)}(z) = \varphi_\ell(z) \tag{A3a}$$

$$f_\ell^{(2)}(z) = \chi_\ell(z) = \frac{1}{\pi}\left[\frac{\partial\varphi_\nu(z)}{\partial\nu} - (-1)^\ell \ \frac{\partial\varphi_{-\nu}(z)}{\partial\nu}\right]_{\nu\to\ell} \tag{A3b}$$

$$f_\ell^{(3)}(z) = \zeta_\ell^{(1)}(z) = \varphi_\ell(z) + \mathrm{i}\chi_\ell(z) \tag{A3c}$$

$$f_\ell^{(4)}(z) = \zeta_\ell^{(2)}(z) = \varphi_\ell(z) - \mathrm{i}\chi_\ell(z). \tag{A3d}$$

A.2. Wronskian

$$W\{\varphi_\nu(z), \varphi_{-\nu}(z)\} = -\sin \nu\pi \tag{A4a}$$

$$W\{\varphi_\nu(z), \chi_\nu(z)\} = 1. \tag{A4b}$$

A.3. Recurrence relations

A complete set of R–B functions can be generated by the recurrence relations:

$$f_{\nu+1}^{(s)}(z) = \frac{(\nu + 1/2)}{z} f_\nu^{(s)}(z) - \frac{\mathrm{d}f_\nu^{(s)}(z)}{\mathrm{d}z} \tag{A5a}$$

$$f_{\nu-1}^{(s)}(z) = \frac{(\nu - 1/2)}{z} f_\nu^{(s)}(z) + \frac{\mathrm{d}f_\nu^{(s)}(z)}{\mathrm{d}z}. \tag{A5b}$$

A.4. Ascending series

(a) When the order ν is not an integer:

$$\varphi_\nu(z) = \sqrt{\pi}\left[\frac{z}{2}\right]^{\frac{1}{2}+\nu}\sum_{p=0}^{\infty}\frac{1}{p!\Gamma(1+p+\nu)}\left[-\frac{z}{4}^2\right]^p \tag{A6a}$$

$$\varphi_{-\nu}(z) = \sqrt{\pi}\left[\frac{z}{2}\right]^{\frac{1}{2}-\nu}\sum_{p=0}^{\infty}\frac{1}{p!\Gamma(1+p-\nu)}\left[-\frac{z}{4}^2\right]^p \tag{A6b}$$

$$\chi_\nu(z) = \frac{\cos\nu\pi\,\varphi_\nu(z) - \varphi_{-\nu}(z)}{\sin\nu\pi}. \tag{A6c}$$

(b) When the order $\nu = \ell$ is an integer:

$$\varphi_\ell(z) = \sqrt{\pi}\left[\frac{z}{2}\right]^{\frac{1}{2}+\ell}\sum_{p=0}^{\infty}\frac{1}{p!(p+\ell)!}\left[-\frac{z^2}{4}\right]^p \tag{A7a}$$

$$\begin{aligned}\chi_\ell(z) = &-\frac{1}{\sqrt{\pi}}\left[\frac{z}{2}\right]^{\frac{1}{2}-\ell}\sum_{p=0}^{\ell-1}\frac{(\ell-p-1)!}{p!}\left[\frac{z^2}{4}\right]^p\\ &+\frac{1}{\sqrt{\pi}}\left[\frac{z}{2}\right]^{\frac{1}{2}+\ell}\sum_{p=0}^{\infty}\frac{\left\{2\ln\left[\frac{z}{2}\right]-\psi(p+1)-\psi(p+\ell+1)\right\}}{p!(p+\ell)!}\left[-\frac{z^2}{4}\right]^p\end{aligned} \tag{A7b}$$

in which $\psi(p)$ is the Digamma function such that $\psi(p) = -\gamma + \sum_{k=1}^{p-1} k^{-1}; p \geqslant 2$ and γ is the Euler–Mascheroni constant.

(c) Specific examples are

$$\begin{aligned}\nu = 0: \quad \varphi_0(z) &= \sqrt{\pi}\left[\frac{z}{2}\right]^{\frac{1}{2}}\sum_{p=0}^{\infty}\frac{\left[\frac{-z^2}{4}\right]^p}{(p!)^2}\\ \chi_0(z) &= \frac{2}{\sqrt{\pi}}\left[\frac{z}{2}\right]^{\frac{1}{2}}\sum_{p=0}^{\infty}\frac{\left\{\ln\left[\frac{z}{2}\right]-\psi(p+1)\right\}}{(p!)^2}\left[-\frac{z^2}{4}\right]^p\end{aligned} \tag{A8a}$$

$$\begin{aligned}\nu = 1: \quad \varphi_1(z) &= \sqrt{\pi}\left[\frac{z}{2}\right]^{\frac{3}{2}}\sum_{p=0}^{\infty}\frac{\left[\frac{-z^2}{4}\right]^p}{p!(p+1)!}\\ \chi_1(z) &= -\frac{1}{\sqrt{\pi}}\left[\frac{z}{2}\right]^{-\frac{1}{2}}+\frac{1}{\sqrt{\pi}}\left[\frac{z}{2}\right]^{\frac{3}{2}}\sum_{p=0}^{\infty}\frac{\left\{2\ln\left[\frac{z}{2}\right]-\psi(p+1)-\psi(p+2)\right\}}{p!(p+1)!}\left[-\frac{z^2}{4}\right]^p.\end{aligned} \tag{A8b}$$

A.5. Asymptotic solutions

When ν is fixed and $z \to \infty$,

$$\varphi_\nu(z) = P_\nu(z)\sin\left[z-\gamma_\nu^0\right] + Q_\nu(z)\cos\left[z-\gamma_\nu^0\right] \tag{A9a}$$

$$\chi_\nu(z) = -P_\nu(z)\cos\left[z-\gamma_\nu^0\right] + Q_\nu(z)\sin\left[z-\gamma_\nu^0\right] \tag{A9b}$$

$$\zeta_\nu^{(1)}(z) = -\mathrm{i}\left[P_\nu(z) + \mathrm{i}Q_\nu(z)\right]\exp\mathrm{i}\left[z-\gamma_\nu^0\right] \tag{A9c}$$

$$\zeta_\nu^{(2)}(z) = \mathrm{i}\,[P_\nu(z) - \mathrm{i}Q_\nu(z)]\exp -\mathrm{i}\left[z - \gamma_\nu^0\right], \tag{A9d}$$

where

$$P_\nu(z) = 1 - \frac{\mu_1\mu_2}{2!(2z)^2} + \frac{\mu_1\mu_2\mu_3\mu_4}{4!(2z)^4} + \cdots \tag{A9e}$$

$$Q_\nu(z) = \frac{\mu_1}{1!(2z)} - \frac{\mu_1\mu_2\mu_3}{3!(2z)^3} + \frac{\mu_1\mu_2\mu_3\mu_4\mu_5}{5!(2z)^5} - \cdots \tag{A9f}$$

and $\mu_0 = 1$, $\mu_s = \nu^2 - (s - 1/2)^2$. Hence

$$\begin{aligned} M_\nu^2(z) &= P_\nu^2(z) + Q_\nu^2(z) \\ &= 1 + \frac{1}{2}\frac{\mu_1}{z^2} + \frac{1\cdot 3}{2\cdot 4}\frac{\mu_1\mu_2}{z^4} + \frac{1\cdot 3\cdot 5}{2\cdot 4\cdot 6}\frac{\mu_1\mu_2\mu_3}{z^6} + \cdots, \end{aligned} \tag{A9g}$$

which is infinite for general order but terminates to become polynomial when the order is half-integer $\nu = \ell + 1/2$.

References

[1] Watson G N 1958 *Treatise on the Theory of Bessel Functions* (Cambridge: Cambridge University Press)
[2] Abramowitz M and Stegun I A 1972 *Handbook of Mathematical Functions* (New York: Dover)
[3] Morse P M and Feshbach H 1953 *Methods of Theoretical Physics* (New York: McGraw-Hill)
[4] Newton R G 1982 *Scattering Theory of Waves and Particles* (New York: Springer)
[5] Grandy W T 2000 *Scattering of Waves from Large Spheres* (Cambridge: Cambridge University Press)
[6] Kerker M 1969 *The Scattering of Light* (New York: Academic)
[7] Jost R and Kohn W 1952 Construction of a potential from a phase shift *Phys. Rev.* **87** 977–92
[8] Chadan K and Sabatier P C 1989 *Inverse Problems in Quantum Scattering Theory* (New York: Springer)
[9] Ludlow I K and Everitt J 2000 Inverse Mie problem *J. Opt. Soc. Am.* A **17** 2229–35
[10] Elbert A 2001 Some recent results on the zeros of Bessel functions and orthogonal polynomials *J. Comput. Appl. Math.* **133** 65–83
[11] Flajolet P and Schott R 1990 Non-overlapping partitions, continued fractions, Bessel functions and a divergent series European *J. Combin.* **11** 421–32
[12] Benton T C and Knoble H D 1978 Common zeros of two Bessel functions *Math. Comp.* **33** 533–5
[13] Benton T C 1983 Common zeros of two Bessel functions: II. Approximation and tables *Math. Comp.* **41** 203–17
[14] Petropoulou E N, Siafarikas P D and Stabolas I D 2003 On the common zeros of Bessel functions *J. Comput. Appl. Math.* **153** 387–93